Electronic Supplementary Material (ESI) for Journal of Materials Chemistry C.

Supporting Information

Efficient Thermally Activated Delayed Fluorescence of Functional Phenylpyridinato Boron Complexes and High Performance Organic Light-Emitting Diodes

Yi-Jiun Shiu,[a,‡] Yi-Ting Chen,[b,‡] Wei-Kai Lee,[a] Chung-Chih Wu,[a,*] Tzu-Chieh Lin,[b] Shih-Hung Liu,[b] Pi-Tai Chou,[b,*] Chin-Wei Lu,[c] I-Chen Cheng,[c] Yi-Jyun Lien,[c] and Yun Chi,[c,*]

[a] Graduate Institute of Electronics Engineering and Department of Electrical Engineering, National Taiwan University, Taipei 10617, Taiwan; E-mail: wucc@ntu.edu.tw

[b] Department of Chemistry, National Taiwan University, Taipei 10617, Taiwan; E-mail: chop@ntu.edu.tw

[c] Department of Chemistry, National Tsing Hua University, Hsinchu 30013, Taiwan; E-mail: ychi@mx.nthu.edu.tw

[‡] Authors with equal contribution.

Tale of content	**page**
Figure X1. Structural drawing, selected bond distances and angles, and crystal data of **fppyBTPA**.	
Figure X2. Structural drawing, selected bond distances and angles, and crystal data of **fppyBPCz**.	
Figure S1 (a). Frontier molecular orbitals pertinent to the optical transitions for **fppyBTPA** in toluene.	
Figure S1 (b). Frontier molecular orbitals pertinent to the optical transitions for **fppyBTPA** in dichloromethane.	
Figure S1 (c). Frontier molecular orbitals pertinent to the optical transitions for **fppyBTPA** in acetonitrile.	
Figure S2 (a). Frontier molecular orbitals pertinent to the optical transitions for **fppyBPCz** in toluene.	
Figure S2 (b). Frontier molecular orbitals pertinent to the optical transitions for	

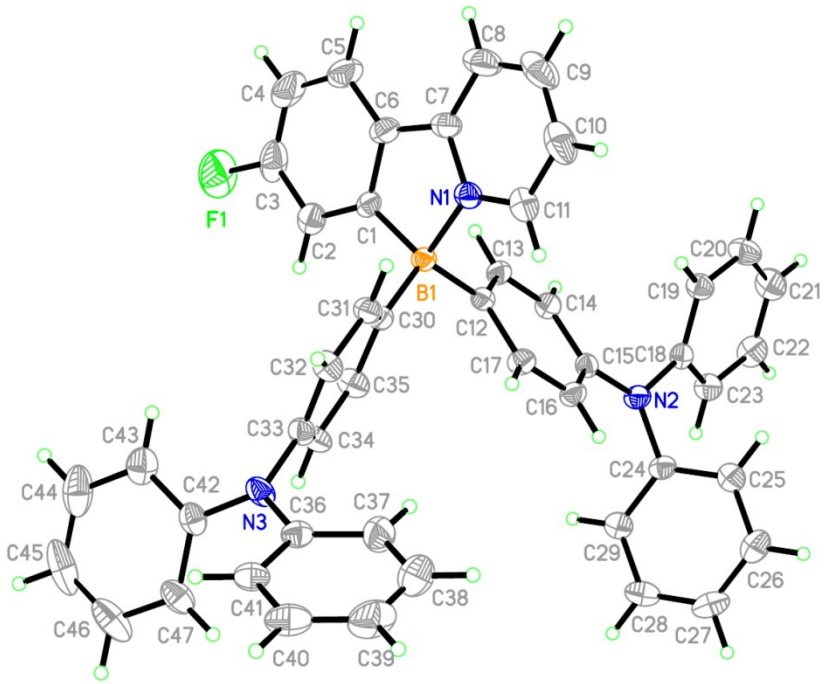

Figure X1. (a) Structural drawing of **fppyBTPA** with thermal ellipsoids shown at 50% probability level. Selected bond distances: B(1)-C(1) = 1.614(2), B(1)-N(1) = 1.624(2), B(1)-C(12) = 1.623(2), B(1)-C(30) 1.610(2) Å, and bond angles: N(1)-B(1)-C(1) = 96.59(11) and C(12)-B(1)-C(30) = 112.55(12)°. Selected crystal data: $C_{47}H_{35}BFN_3$; M = 671.59; T = 200(2) K; triclinic; space group = P–1; *a* = 9.7399(5) Å, *b* = 13.7142(8) Å, *c* = 14.6944(8) Å; α = 101.835(3)°, β = 95.538(2)°, γ = 110.288(2)°, *V* = 1771.61(17) Å^3; *Z* = 2; ρ_{calcd} = 1.259 Mg·m^{-3}; *F*(000) = 704; μ = 0.077 mm^{-1}; crystal size = 0.200 × 0.150 × 0.070 mm^3; λ(Mo-K$_\alpha$) = 0.71073 Å; 16238 reflections collected, 8134 independent reflections (R_{int} = 0.0195), restraints / parameters = 0 / 469, GOF = 1.008, final $R_1[I > 2\sigma(I)]$ = 0.0515 and wR_2(all data) = 0.1399; largest diff. peak and hole = 1.092 and -0.490 e·Å^{-3}. Comprehensive structural information: CCDC 1517425.

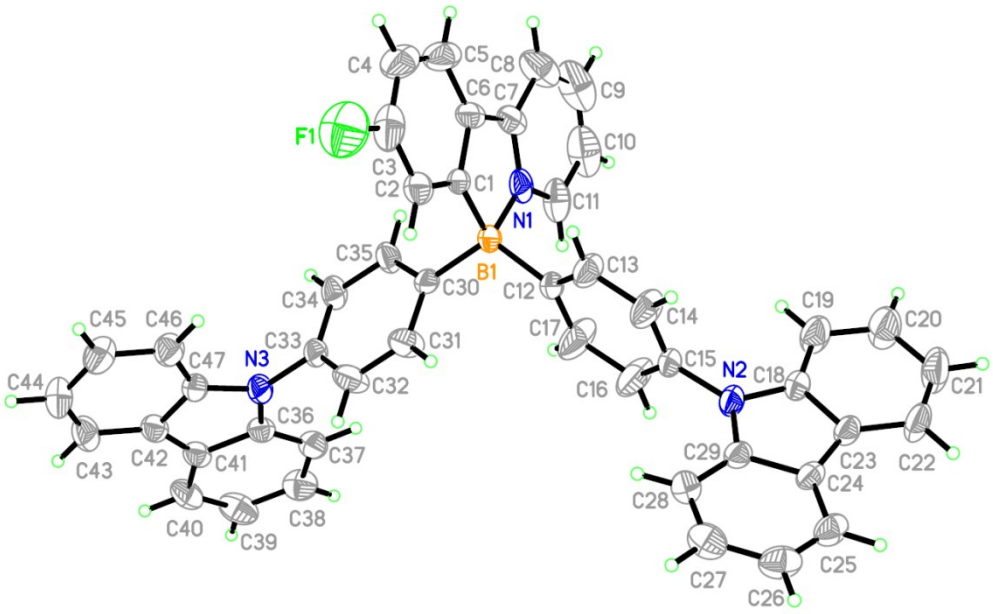

Figure X2. (a) Structural drawing of **fppyBPCz** with thermal ellipsoids shown at 50% probability level. Selected bond distances: B(1)-C(1) = 1.620(5), B(1)-N(1) = 1.626(5), B(1)-C(12) = 1.617(5), B(1)-C(30) 1.622(5) Å, and bond angles: N(1)-B(1)-C(1) = 96.8(2) and C(12)-B(1)-C(30) = 114.7(3)°. Selected crystal data: $C_{47}H_{31}BFN_3$; M = 667.56; T = 200(2) K; monoclinic; space group = C_C; *a* = 22.2980(9) Å, *b* = 12.8948(5) Å, *c* = 16.2166(6) Å; β = 131.7267(13)°, *V* = 3479.9(2) Å^3; *Z* = 4; ρ_{calcd} = 1.274 Mg·m^{-3}; *F*(000) = 1392; μ = 0.610 mm^{-1}; crystal size = 0.250 × 0.200 × 0.200 mm^3; λ(Mo-K$_\alpha$) = 0.71073 Å; 11879 reflections collected, 6539 independent reflections (R_{int} = 0.0257), restraints / parameters = 2 / 470, GOF = 1.048, final $R_1[I > 2\sigma(I)]$ = 0.0481 and wR_2(all data) = 0.1381; largest diff. peak and hole = 0.826 and -0.369 e·Å^{-3}. Comprehensive structural information: CCDC 1517424.

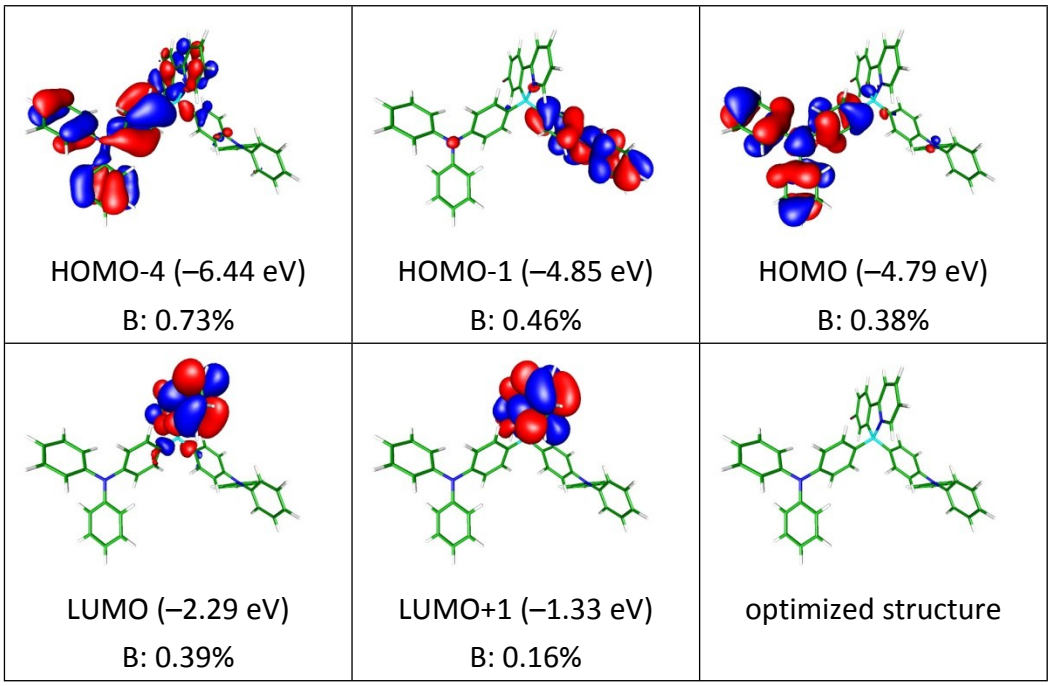

Figure S1 (a). Frontier molecular orbitals pertinent to the optical transitions for **fppyBTPA** in toluene.

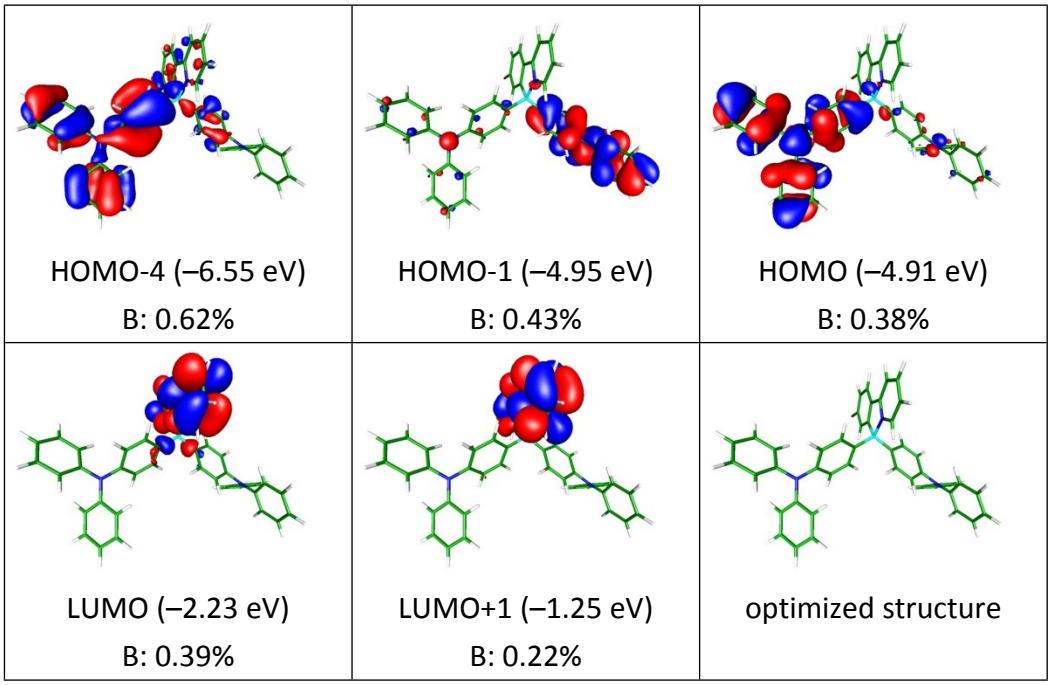

Figure S1 (b). Frontier molecular orbitals pertinent to the optical transitions for **fppyBTPA** in dichloromethane.

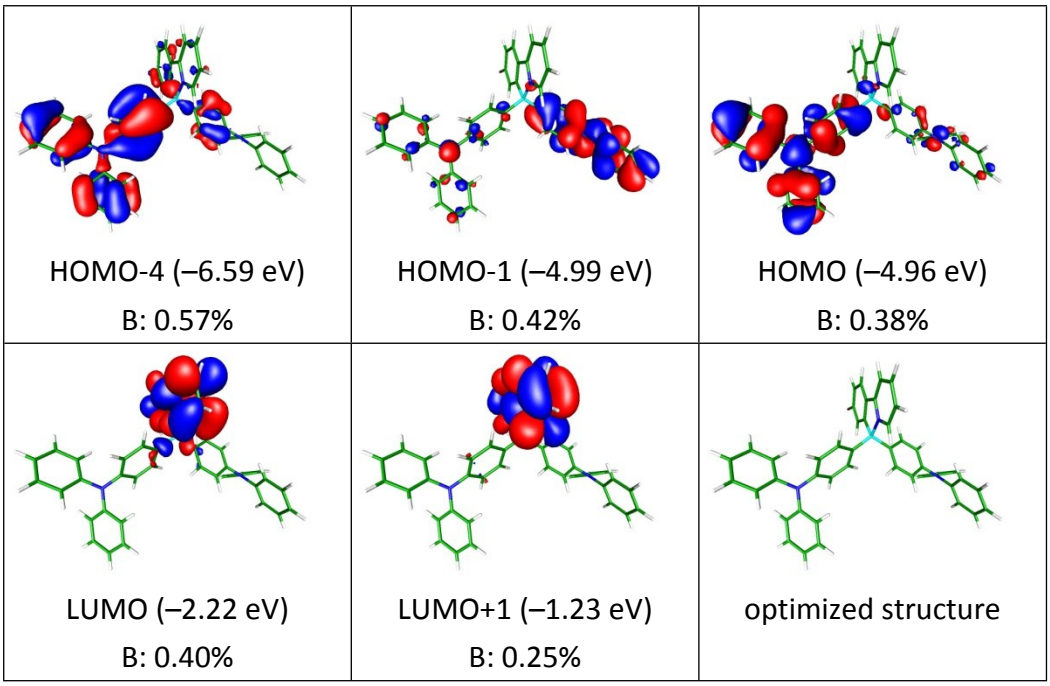

Figure S1 (c). Frontier molecular orbitals pertinent to the optical transitions for **fppyBTPA** in acetonitrile.

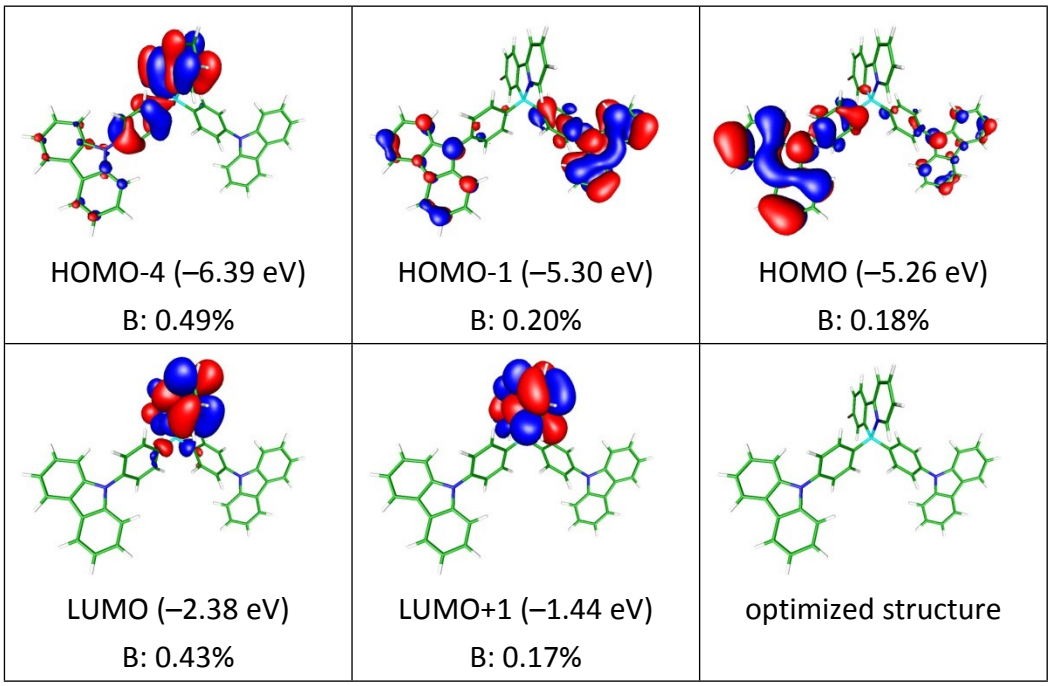

Figure S2 (a). Frontier molecular orbitals pertinent to the optical transitions for **fppyBPCz** in toluene.

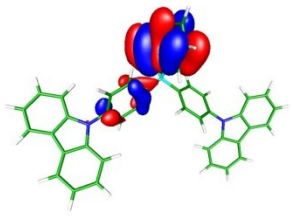 HOMO-4 (–6.35 eV) B: 0.36%	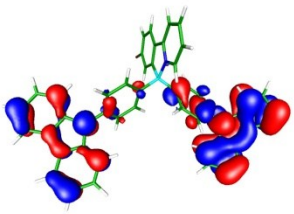 HOMO-1 (–5.41 eV) B: 0.19%	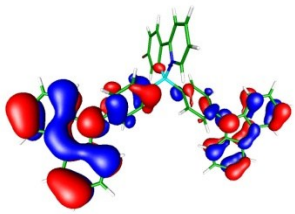 HOMO (–5.37 eV) B: 0.20%
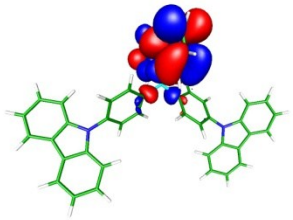 LUMO (–2.06 eV) B: 0.44%	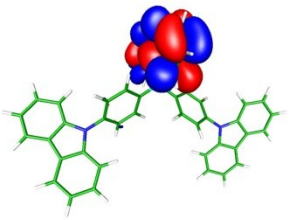 LUMO+1 (–1.31 eV) B: 0.23%	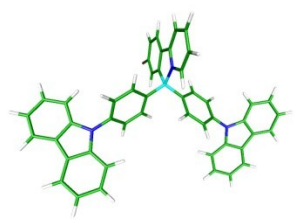 optimized structure

Figure S2 (b). Frontier molecular orbitals pertinent to the optical transitions for **fppyBPCz** in dichloromethane.

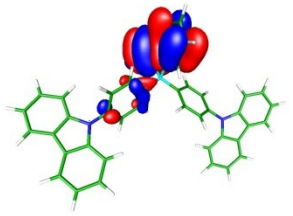 HOMO-4 (–6.34 eV) B: 0.34%	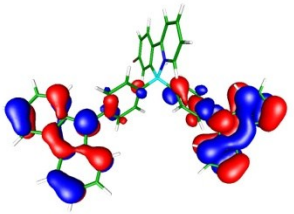 HOMO-1 (–5.45 eV) B: 0.18%	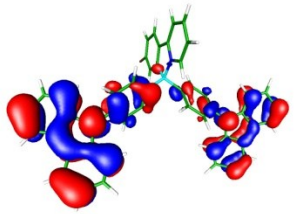 HOMO (–5.41 eV) B: 0.20%
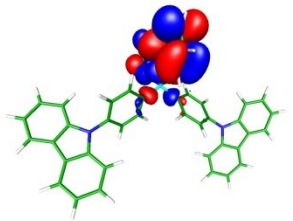 LUMO (–2.23 eV) B: 0.45%	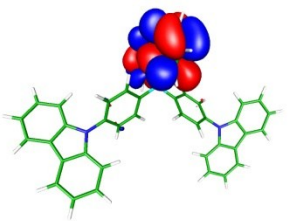 LUMO+1 (–1.27 eV) B: 0.27%	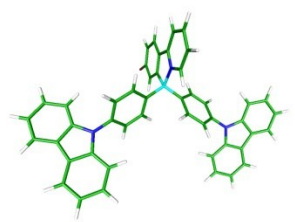 optimized structure

Figure S2 (c). Frontier molecular orbitals pertinent to the optical transitions for **fppyBPCz** in acetonitrile.

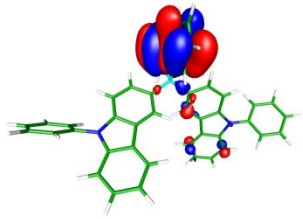 HOMO-4 (–6.24 eV) B: 0.34%	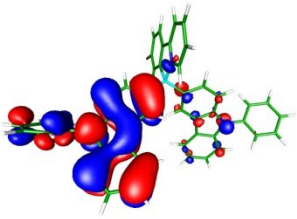 HOMO-1 (–5.17 eV) B: 0.53%	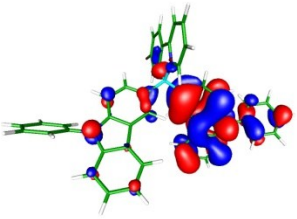 HOMO (–5.08 eV) B: 0.60%
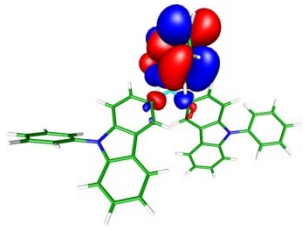 LUMO (–2.28 eV) B: 0.37%	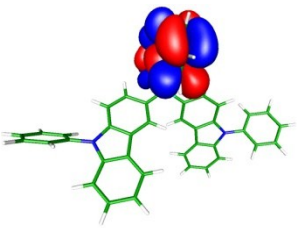 LUMO+1 (–1.26 eV) B: 0.17%	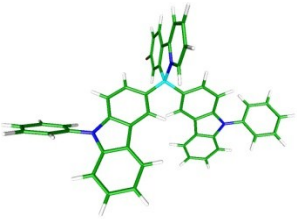 optimized structure

Figure S3 (a). Frontier molecular orbitals pertinent to the optical transitions for **fppyBCzP** in toluene.

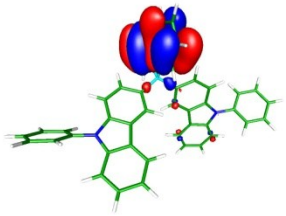 HOMO-4 (–6.28 eV) B: 0.32%	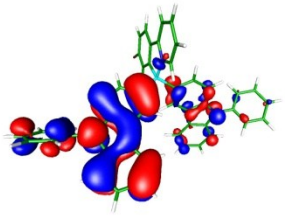 HOMO-1 (–5.31 eV) B: 0.49%	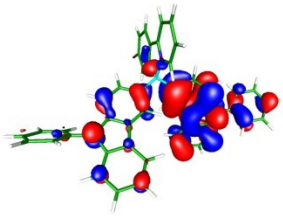 HOMO (–5.22 eV) B: 0.60%
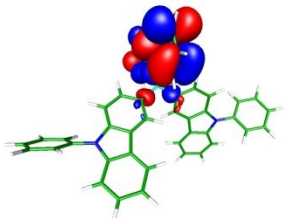 LUMO (–2.26 eV) B: 0.38%	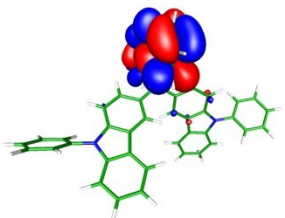 LUMO+1 (–1.22 eV) B: 0.24%	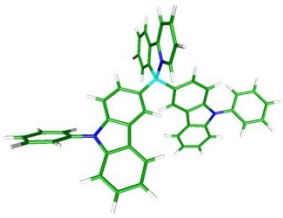 optimized structure

Figure S3 (b). Frontier molecular orbitals pertinent to the optical transitions for **fppyBCzP** in dichloromethane.

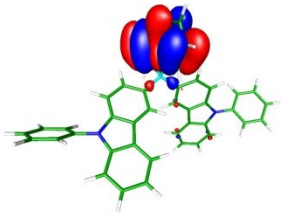 HOMO-4 (–6.30 eV) B: 0.31%	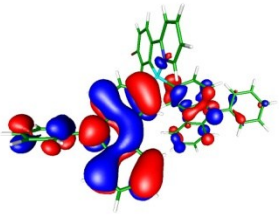 HOMO-1 (–5.36 eV) B: 0.48%	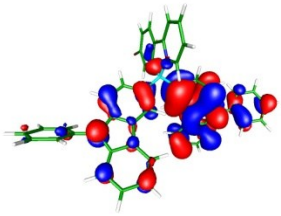 HOMO (–5.27 eV) B: 0.60%
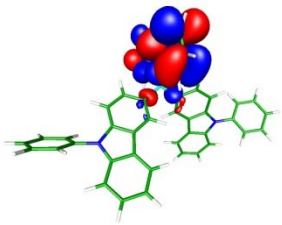 LUMO (–2.25 eV) B: 0.38%	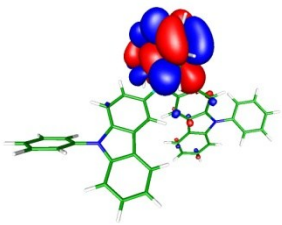 LUMO+1 (–1.22 eV) B: 0.27%	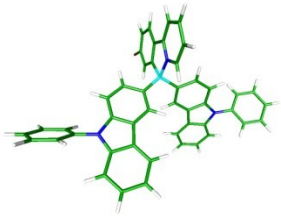 optimized structure

Figure S3 (c). Frontier molecular orbitals pertinent to the optical transitions for **fppyBCzP** in acetonitrile.

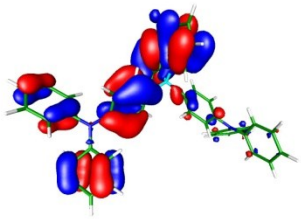 HOMO-4 (–6.49 eV) B: 0.38%	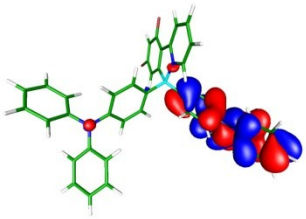 HOMO-1 (–4.87 eV) B: 0.47%	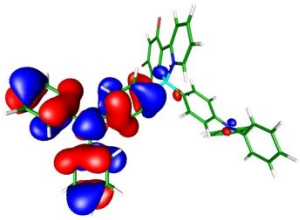 HOMO (–4.82 eV) B: 0.38%
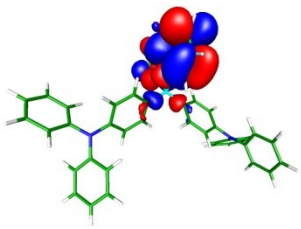 LUMO (–2.36 eV) B: 0.37%	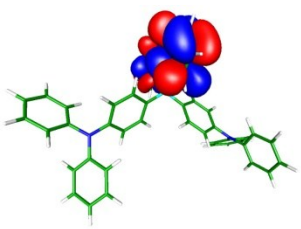 LUMO+1 (–1.32 eV) B: 0.13%	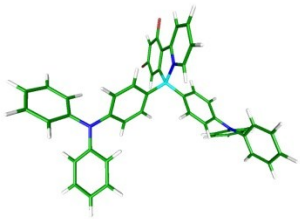 optimized structure

Figure S4 (a). Frontier molecular orbitals pertinent to the optical transitions for **dfppyBTPA** in toluene.

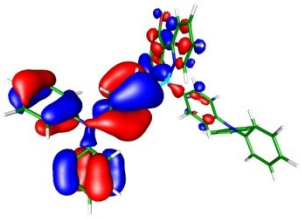 HOMO-4 (–6.57 eV) B: 0.46%	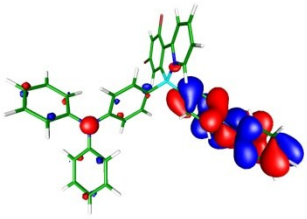 HOMO-1 (–4.97 eV) B: 0.44%	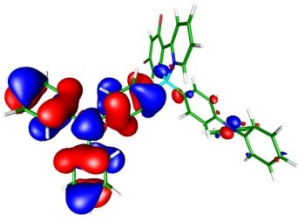 HOMO (–4.93 eV) B: 0.39%
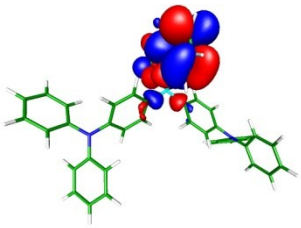 LUMO (–2.31 eV) B: 0.38%	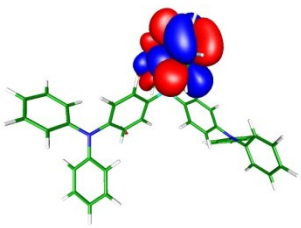 LUMO+1 (–1.25 eV) B: 0.18%	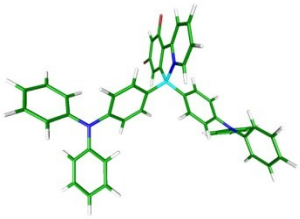 optimized structure

Figure S4 (b). Frontier molecular orbitals pertinent to the optical transitions for **dfppyBTPA** in dichloromethane.

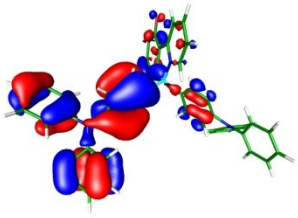 HOMO-4 (–6.61 eV) B: 0.43%	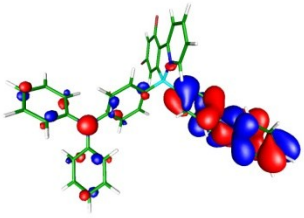 HOMO-1 (–5.00 eV) B: 0.42%	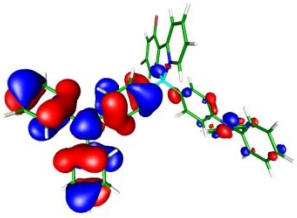 HOMO (–4.97 eV) B: 0.39%
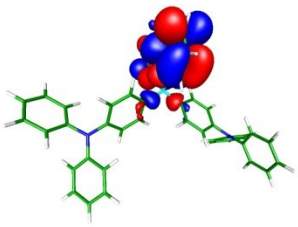 LUMO (–2.29 eV) B: 0.38%	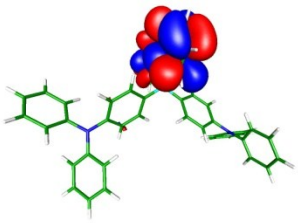 LUMO+1 (–1.23 eV) B: 0.20%	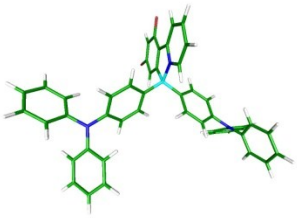 optimized structure

Figure S4 (c). Frontier molecular orbitals pertinent to the optical transitions for **dfppyBTPA** in acetonitrile.

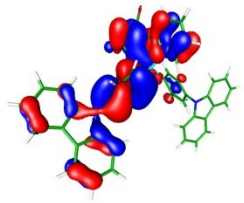 HOMO-4 (–6.53 eV) B: 0.90%	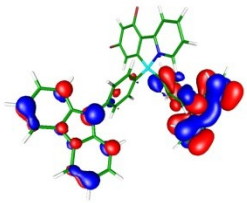 HOMO-1 (–5.32 eV) B: 0.20%	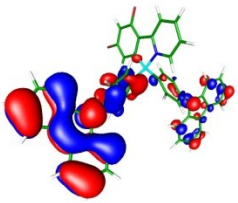 HOMO (–5.28 eV) B: 0.18%
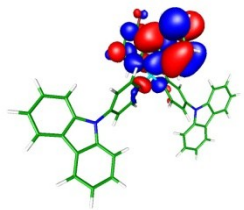 LUMO (–2.45 eV) B: 0.41%	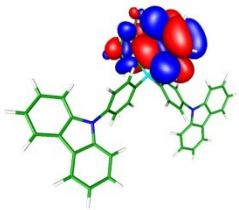 LUMO+1 (–1.45 eV) B: 0.14%	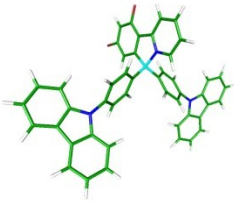 optimized structure

Figure S5 (a). Frontier molecular orbitals pertinent to the optical transitions for **dfppyBPCz** in toluene.

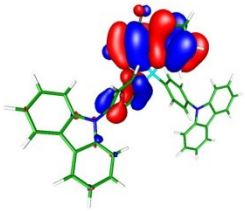 HOMO-4 (–6.50 eV) B: 0.29%	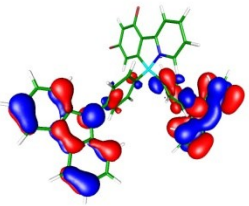 HOMO-1 (–5.42 eV) B: 0.19%	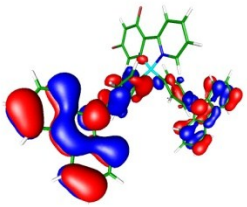 HOMO (–5.38 eV) B: 0.19%
 LUMO (–2.34 eV) B: 0.42%	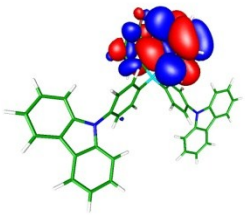 LUMO+1 (–1.31 eV) B: 0.19%	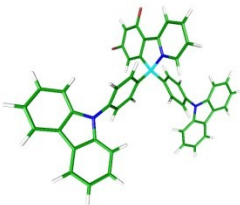 optimized structure

Figure S5 (b). Frontier molecular orbitals pertinent to the optical transitions for **dfppyBPCz** in dichloromethane.

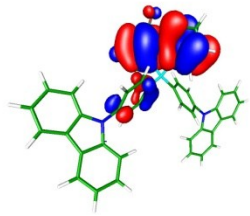 HOMO-4 (–6.49 eV) B: 0.22%	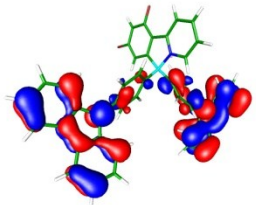 HOMO-1 (–5.46 eV) B: 0.18%	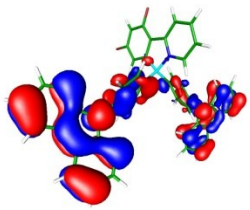 HOMO (–5.42 eV) B: 0.20%
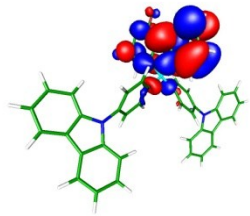 LUMO (–2.30 eV) B: 0.43%	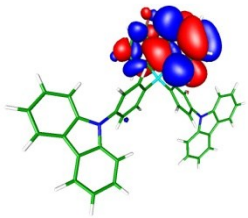 LUMO+1 (–1.27 eV) B: 0.21%	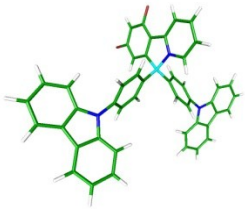 optimized structure

Figure S5 (c). Frontier molecular orbitals pertinent to the optical transitions for **dfppyBPCz** in acetonitrile.

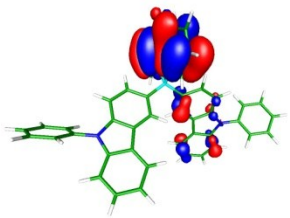 HOMO-4 (–6.40 eV) B: 0.18%	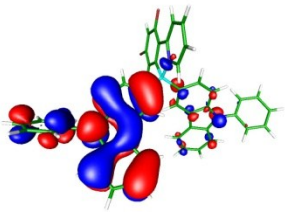 HOMO-1 (–5.20 eV) B: 0.54%	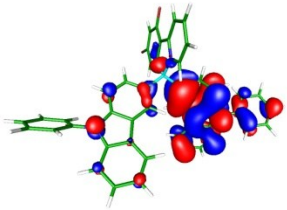 HOMO (–5.11 eV) B: 0.59%
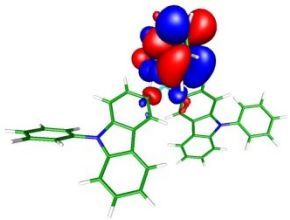 LUMO (–2.34 eV) B: 0.35%	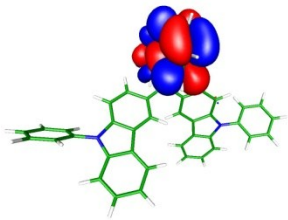 LUMO+1 (–1.26 eV) B: 0.15%	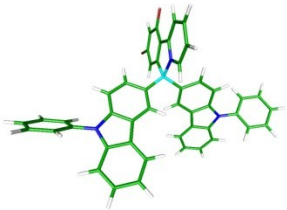 optimized structure

Figure S6 (a). Frontier molecular orbitals pertinent to the optical transitions for **dfppyBCzP** in toluene.

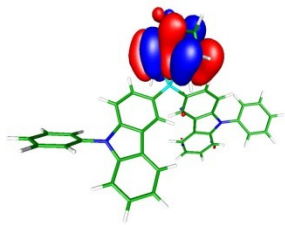 HOMO-4 (–6.43 eV) B: 0.14%	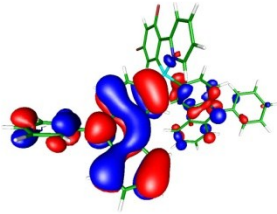 HOMO-1 (–5.33 eV) B: 0.50%	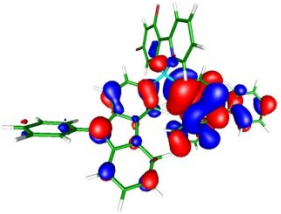 HOMO (–5.24 eV) B: 0.59%
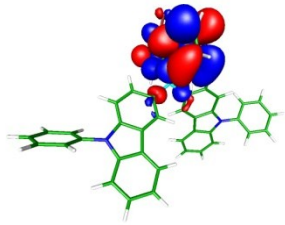 LUMO (–2.33 eV) B: 0.36%	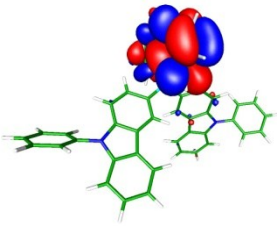 LUMO+1 (–1.23 eV) B: 0.20%	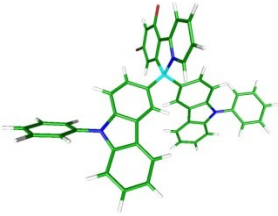 optimized structure

Figure S6 (b). Frontier molecular orbitals pertinent to the optical transitions for **dfppyBCzP** in dichloromethane.

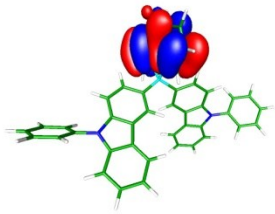 HOMO-4 (–6.44 eV) B: 0.14%	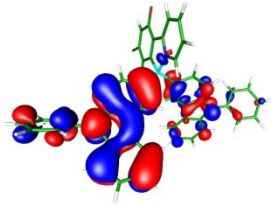 HOMO-1 (–5.38 eV) B: 0.48%	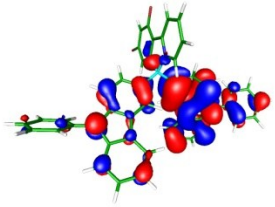 HOMO (–5.29 eV) B: 0.59%
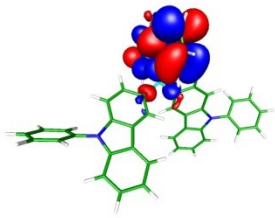 LUMO (–2.32 eV) B: 0.36%	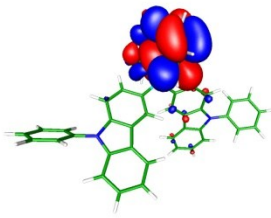 LUMO+1 (–1.22 eV) B: 0.22%	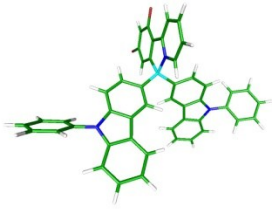 optimized structure

Figure S6 (c). Frontier molecular orbitals pertinent to the optical transitions for **dfppyBCzP** in acetonitrile.

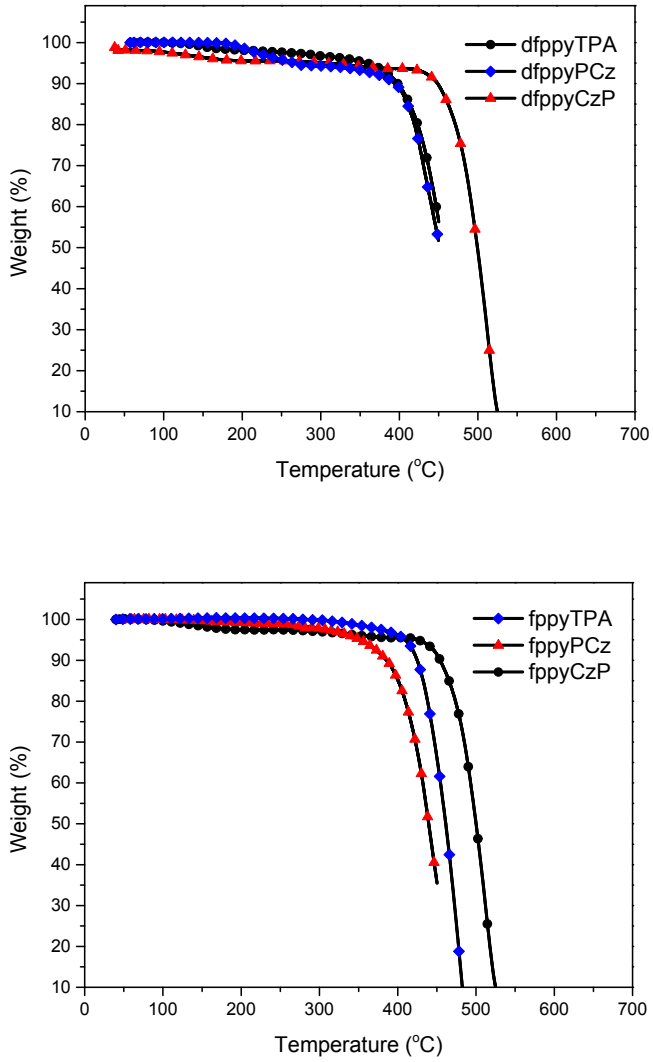

Figure S7. TGA data of **fppyBTPA**, **fppyBPCz**, **fppyBCzP**, **dfppyBTPA**, **dfppyBPCz**, and **dfppyBCzP**. The samples were heated under a nitrogen atmosphere at a heating rate of 15 °C/min.

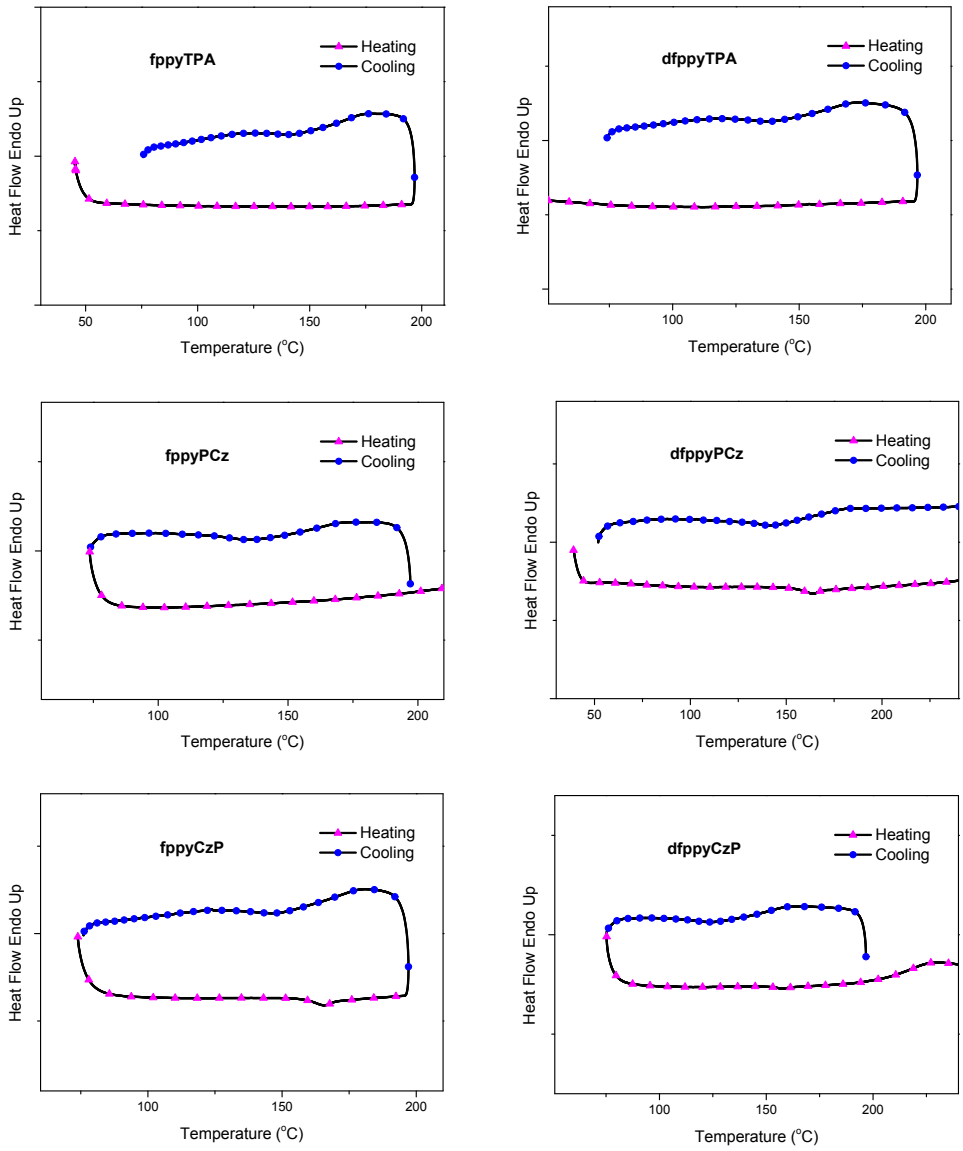

Figure S8. DSC data of **fppyBTPA**, **fppyBPCz**, **fppyBCzP**, **dfppyBTPA**, **dfppyBPCz**, and **dfppyBCzP**. The samples were heated and cooled under a nitrogen atmosphere at a rate of 10 °C/min.

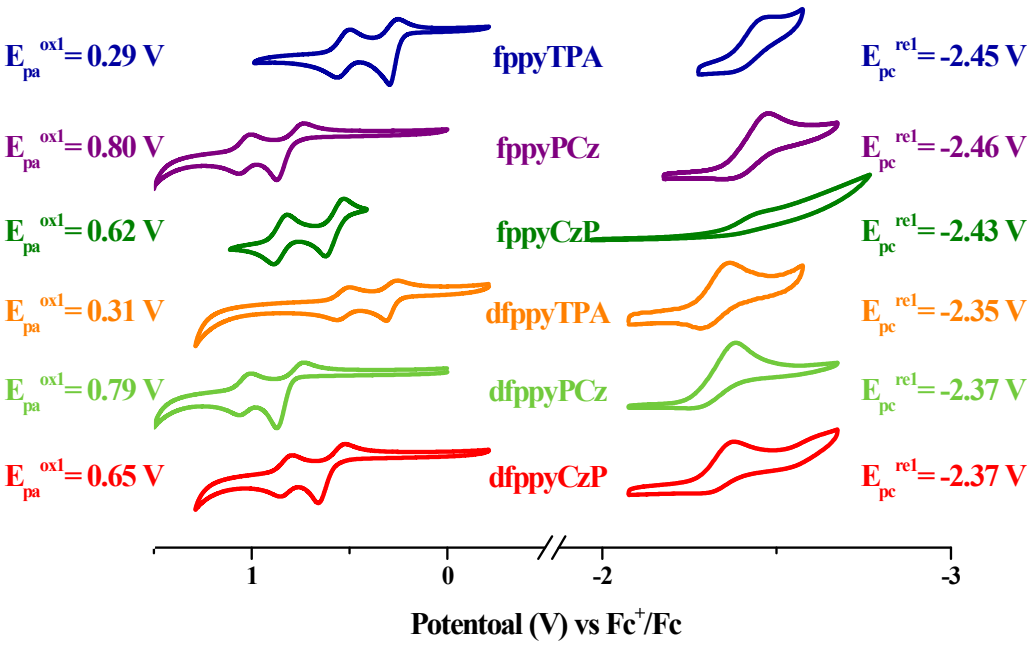

Figure S9. Cyclic voltammograms of **fppyBTPA**, **fppyBPCz**, **fppyBCzP**, **dfppyBTPA**, **dfppyBPCz**, and **dfppyBCzP**. The oxidation and reduction experiments were conducted in CH_2Cl_2 and acetonitrile solution, respectively. The glassy carbon was selected as the working electrode for both oxidation and reduction processes.

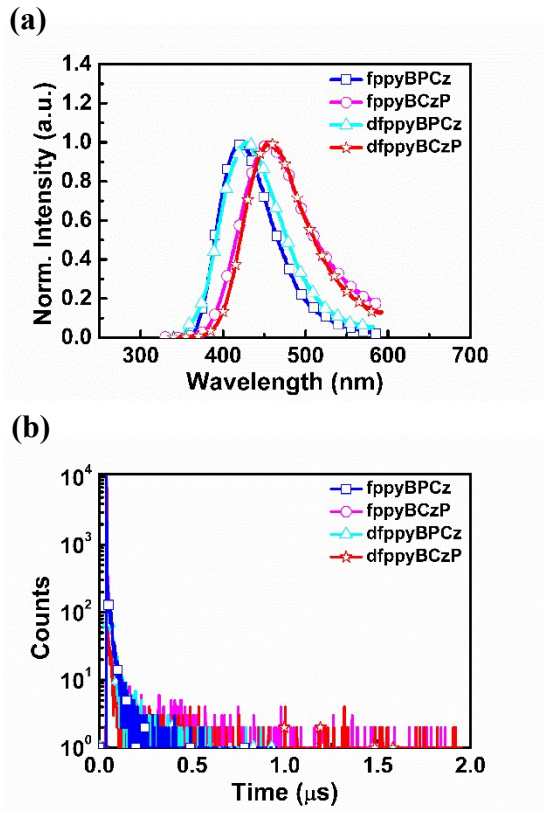

Figure S10. (a) PL spectra and (b) transient PL profiles (measured at room temperature) of **fppyBPCz, fppyBCzP**, **dfppyBPCz** and **dfppyBCzP** doped (with 8 wt.% concentration) in the DPEPO host.

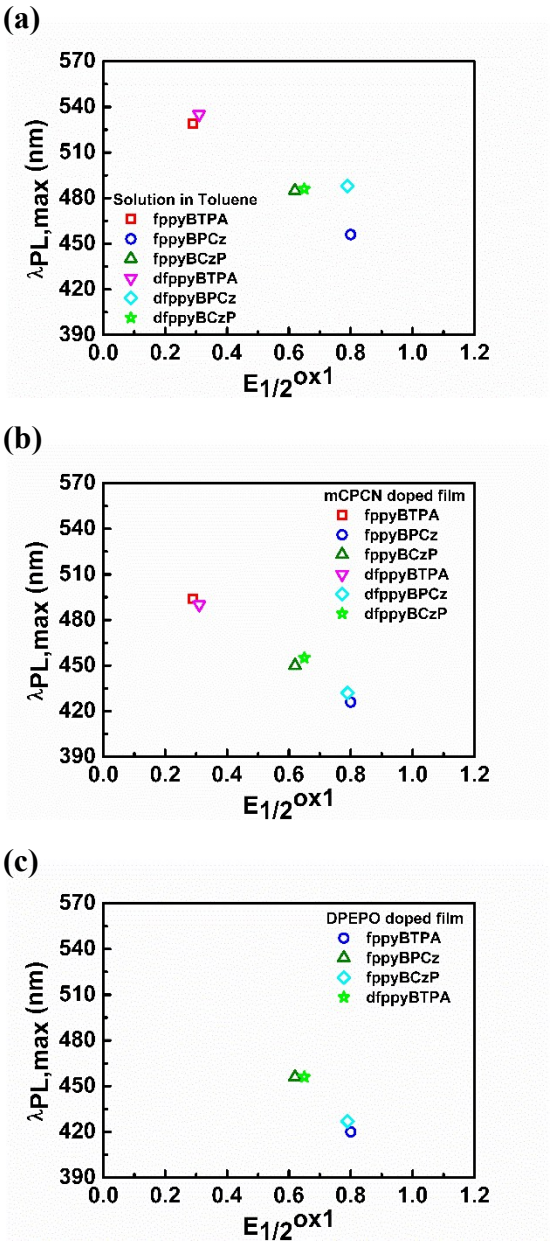

Figure S11. PL peak wavelengths vs. oxidation potential for compounds in (a) toluene solution, (b) doped mCPCN films, and (c) doped DPEPO films.

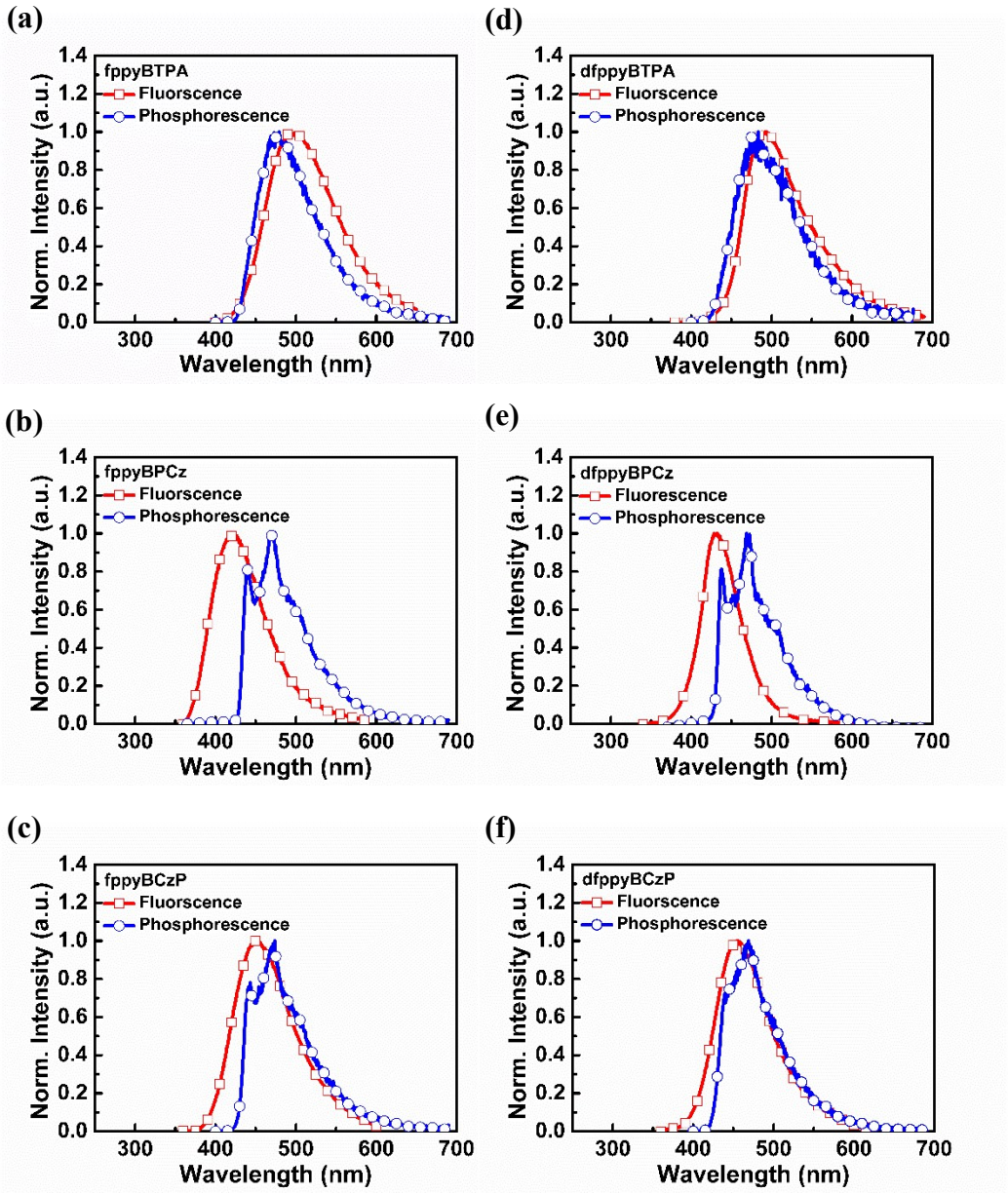

Figure S12. PL spectra (measured at room temperature) and phosphorescence spectra (measured at 77 K) of (a) **fppyBTPA**, (b) **fppyBPCz**, (c) **fppyBCzP,** (d) **dfppyBTPA**, **(e) dfppyBPCz** and (f) **dfppyBCzP** doped in the mCPCN host (with 8 wt.% concentration).

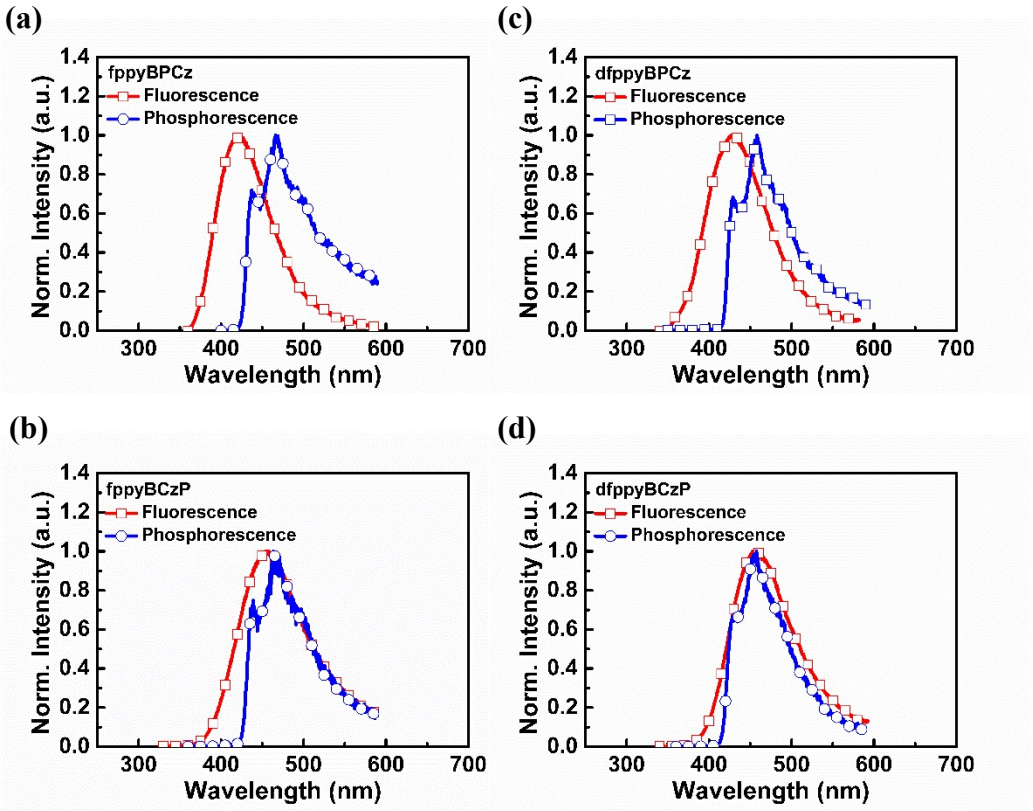

Figure S13. PL spectra (measured at room temperature) and phosphorescence spectra (measured at 77 K) of (a) **fppyBPCz,** (b) **fppyBCzP**, (c) **dfppyBPCz** and (d) **dfppyBCzP** doped in the DPEPO host (with 8 wt.% concentration).

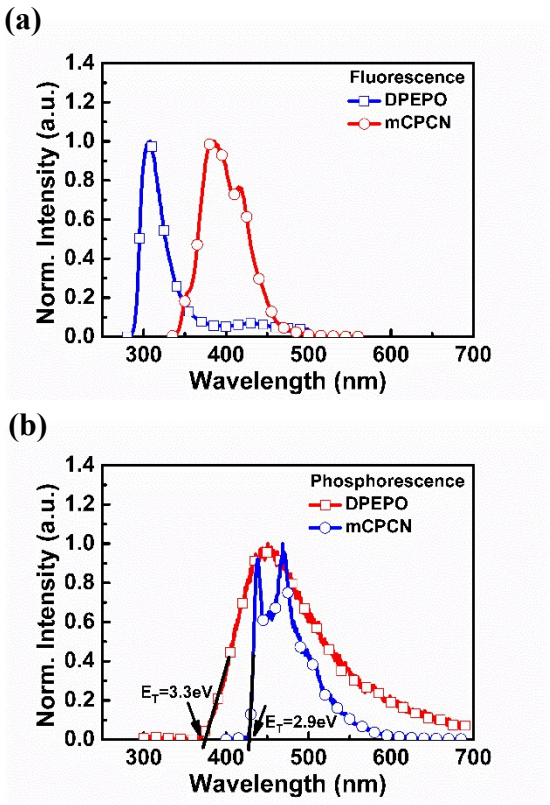

Figure S14. (a) PL spectra (measured at room temperature) and (b) phosphorescence spectra (measured at 77 K) of neat mCPCN and DPEPO films.

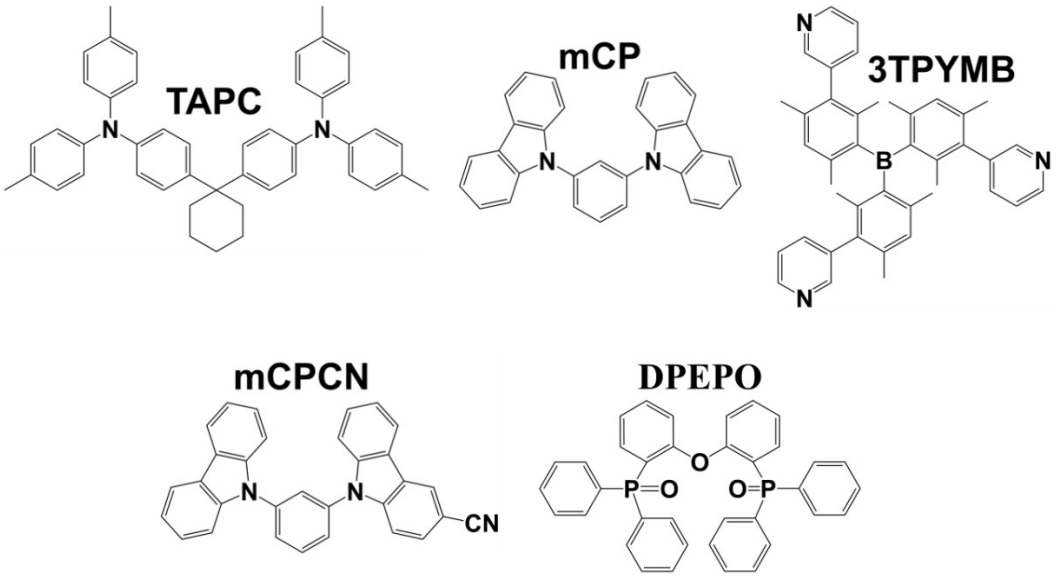

Figure S15. Molecular structures of materials used in OLEDs and thin-film samples.

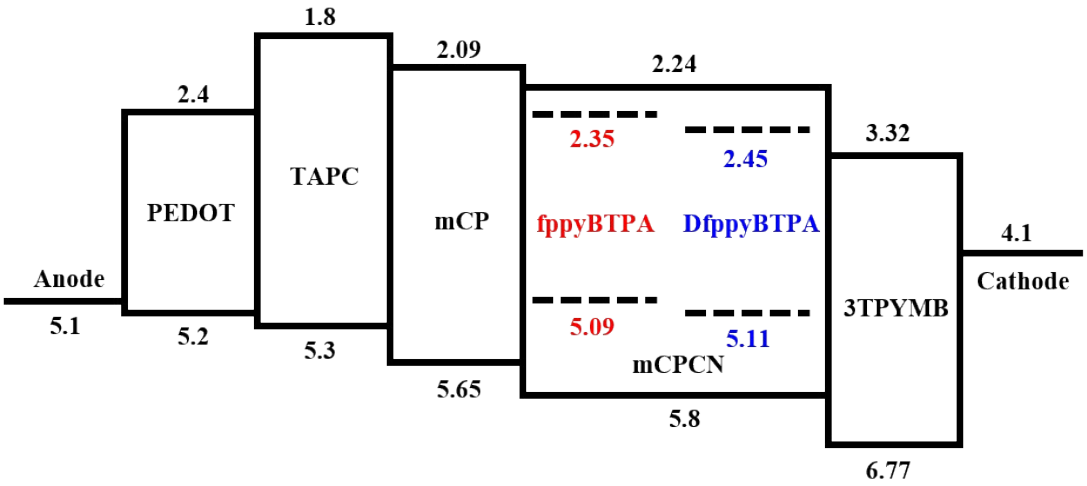

Figure S16. Relative energy levels of various materials used in OLEDs.

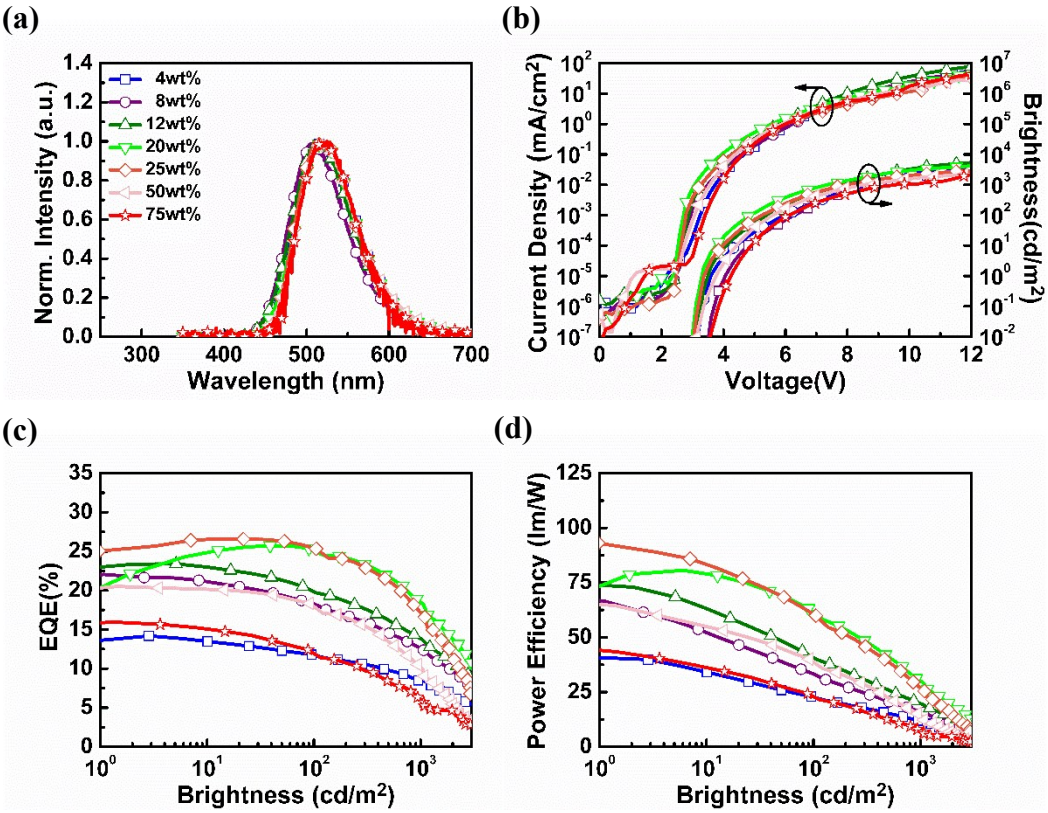

Figure S17. (a) EL spectra and (b) current-voltage-luminance (I-V-L) characteristics, (c) external quantum efficiencies (EQEs), and (d) power efficiencies of the **dfppyBTPA** devices with different **dfppyBTPA** doping concentrations.

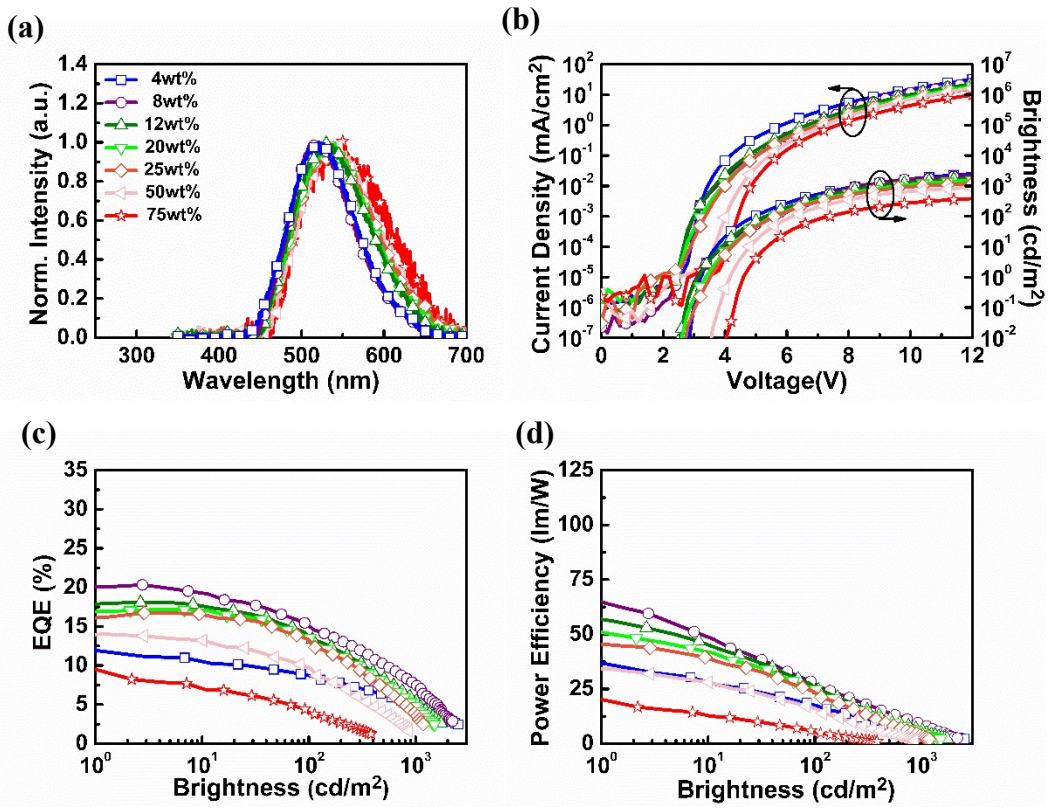

Figure S18. (a) EL spectra and (b) current-voltage-luminance (I-V-L) characteristics, (c) external quantum efficiencies (EQEs), and (d) power efficiencies of the **fppyBTPA** devices with different **fppyBTPA** doping concentrations.

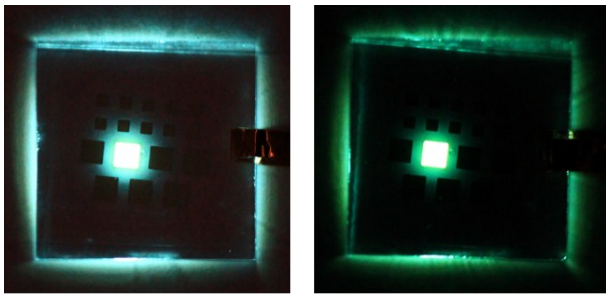

Figure S19. Photos of the operating (a) **fppyBTPA** (8 wt.%) and (b) **dfppyBTPA** (25 wt.%) devices.

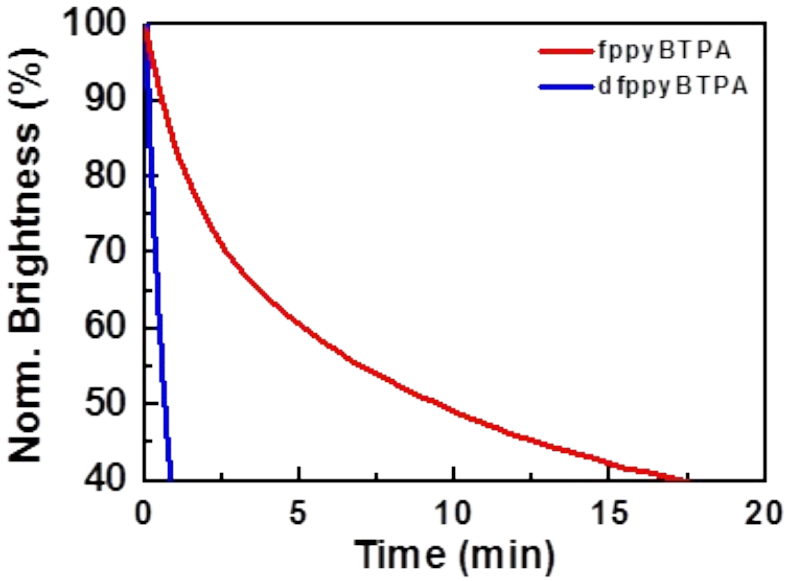

Figure S20. The time-dependent brightess in % under an initial brightness of 200-250 cd·m^{-2} for fppyBTPA and dfppyBTPA

Table S1 (a). The calculated wavelengths, transition probabilities and charge transfer character of the lowest optical transitions for **fppyBTPA** in toluene.

State	λ (nm)	f	Assignments
$S_0 \rightarrow T_1$	500.1	0	HOMO → LUMO (97%)
$S_0 \rightarrow S_1$	496.2	0.0057	HOMO → LUMO (99%)

Table S1 (b). The calculated wavelengths, transition probabilities and charge transfer character of the lowest optical transitions for **fppyBTPA** in dichloromethane.

State	λ (nm)	f	Assignments
$S_0 \rightarrow T_1$	467.1	0	HOMO → LUMO (94%)
$S_0 \rightarrow S_1$	463.1	0.0062	HOMO → LUMO (98%)

Table S1 (c). The calculated wavelengths, transition probabilities and charge transfer character of the lowest optical transitions for **fppyBTPA** in acetonitrile.

State	λ (nm)	f	Assignments
$S_0 \rightarrow T_1$	456.9	0	HOMO → LUMO (92%)
$S_0 \rightarrow S_1$	452.7	0.0062	HOMO → LUMO (98%)

Table S2 (a). The calculated wavelengths, transition probabilities and charge transfer character of the lowest optical transitions for **fppyBPCz** in toluene.

State	λ (nm)	f	Assignments
$S_0 \rightarrow T_1$	433.5	0	HOMO → LUMO (94%)
$S_0 \rightarrow S_1$	430.9	0.0036	HOMO → LUMO (98%)

Table S2 (b). The calculated wavelengths, transition probabilities and charge transfer character of the lowest optical transitions for **fppyBPCz** in dichloromethane.

State	λ (nm)	f	Assignments
$S_0 \rightarrow T_1$	416.4	0	HOMO-4 → LUMO (66%) HOMO-4 → LUMO+1 (11%)
$S_0 \rightarrow S_1$	399.3	0.0045	HOMO → LUMO (98%)

Table S2 (c). The calculated wavelengths, transition probabilities and charge transfer character of the lowest optical transitions for **fppyBPCz** in acetonitrile.

State	λ (nm)	f	Assignments
$S_0 \rightarrow T_1$	414.8	0	HOMO-4 LUMO (68%) HOMO-4 LUMO+1 (11%)
$S_0 \rightarrow S_1$	389.9	0.0048	HOMO → LUMO (98%)

Table S3 (a). The calculated wavelengths, transition probabilities and charge transfer character of the lowest optical transitions for **fppyBCzP** in toluene.

State	λ (nm)	f	Assignments
$S_0 \rightarrow T_1$	447.9	0	HOMO → LUMO (94%)
$S_0 \rightarrow S_1$	442.1	0.0057	HOMO → LUMO (98%)

Table S3 (b). The calculated wavelengths, transition probabilities and charge transfer character of the lowest optical transitions for **fppyBCzP** in dichloromethane.

State	λ (nm)	f	Assignments
$S_0 \rightarrow T_1$	425.5	0	HOMO → LUMO (73%) HOMO-4 → LUMO (15%)
$S_0 \rightarrow S_1$	418.4	0.007	HOMO → LUMO (98%)

Table S3 (c). The calculated wavelengths, transition probabilities and charge transfer character of the lowest optical transitions for **fppyBCzP** in acetonitrile.

State	λ (nm)	f	Assignments
$S_0 \rightarrow T_1$	419.7	0	HOMO → LUMO (38%) HOMO-4 → LUMO (35%) HOMO-1 → LUMO (10%) HOMO-4 → LUMO+1 (6%)
$S_0 \rightarrow S_1$	410.3	0.0072	HOMO → LUMO (98%)

Table S4 (a). The calculated wavelengths, transition probabilities and charge transfer character of the lowest optical transitions for **dfppyBTPA** in toluene.

State	λ (nm)	f	Assignments
$S_0 \rightarrow T_1$	508.8	0	HOMO → LUMO (96%)
$S_0 \rightarrow S_1$	504.9	0.0063	HOMO → LUMO (99%)

Table S4 (b). The calculated wavelengths, transition probabilities and charge transfer character of the lowest optical transitions for **dfppyBTPA** in dichloromethane.

State	λ (nm)	f	Assignments
$S_0 \rightarrow T_1$	477.2	0	HOMO → LUMO (94%)
$S_0 \rightarrow S_1$	473	0.0068	HOMO → LUMO (98%)

Table S4 (c). The calculated wavelengths, transition probabilities and charge transfer character of the lowest optical transitions for **dfppyBTPA** in acetonitrile.

State	λ (nm)	f	Assignments
$S_0 \rightarrow T_1$	467.1	0	HOMO → LUMO (92%) HOMO-1 → LUMO (5%)
$S_0 \rightarrow S_1$	462.8	0.0067	HOMO → LUMO (98%)

Table S5 (a). The calculated wavelengths, transition probabilities and charge transfer character of the lowest optical transitions for **dfppyBPCz** in toluene.

State	λ (nm)	f	Assignments
$S_0 \rightarrow T_1$	441	0	HOMO → LUMO (95%)
$S_0 \rightarrow S_1$	438.7	0.0039	HOMO → LUMO (98%)

Table S5 (b). The calculated wavelengths, transition probabilities and charge transfer character of the lowest optical transitions for **dfppyBPCz** in dichloromethane.

State	λ (nm)	f	Assignments
$S_0 \rightarrow T_1$	411.4	0	HOMO → LUMO (41%) HOMO-4 → LUMO (39%) HOMO-1 → LUMO (7%) HOMO-4 → LUMO+1 (5%)
$S_0 \rightarrow S_1$	407.4	0.0047	HOMO → LUMO (98%)

Table S5 (c). The calculated wavelengths, transition probabilities and charge transfer character of the lowest optical transitions for **dfppyBPCz** in acetonitrile.

State	λ (nm)	f	Assignments
$S_0 \rightarrow T_1$	408.8	0	HOMO-4 → LUMO (66%) HOMO-4 → LUMO+1 (10%) HOMO-1 → LUMO (7%)
$S_0 \rightarrow S_1$	397.9	0.0049	HOMO → LUMO (98%)

Table S6 (a). The calculated wavelengths, transition probabilities and charge transfer character of the lowest optical transitions for **dfppyBCzP** in toluene.

State	λ (nm)	f	Assignments
$S_0 \rightarrow T_1$	453.3	0	HOMO → LUMO (96%)
$S_0 \rightarrow S_1$	447.9	0.0065	HOMO → LUMO (98%)

Table S6 (b). The calculated wavelengths, transition probabilities and charge transfer character of the lowest optical transitions for **dfppyBCzP** in dichloromethane.

State	λ (nm)	f	Assignments
$S_0 \rightarrow T_1$	431	0	HOMO → LUMO (94%)
$S_0 \rightarrow S_1$	425.5	0.0077	HOMO → LUMO (98%)

Table S6 (c). The calculated wavelengths, transition probabilities and charge transfer character of the lowest optical transitions for **dfppyBCzP** in acetonitrile.

State	λ (nm)	f	Assignments
$S_0 \rightarrow T_1$	423.4	0	HOMO → LUMO (92%)
$S_0 \rightarrow S_1$	417.7	0.0078	HOMO → LUMO (98%)

Table S7. Photophysical properties of the complexes in CH_2Cl_2 and CH_3CN at room temperature.

Compound	CT [nm]	PLQY [%]	τ_{CT} [ns][b] (pre-exp factor)	$\Delta E_{T\text{-}S}$ [kcal/mol]
		In DCM		
fppyBTPA	600	11.1[a], 13.1[b]	29.6(–)	
fppyBPCz	508	16.1[a], 60.7[b]	118.2 (–)	
fppyBCzP	519	20.2[a], 56.0[b]	58.6 (–)	
dfppyBTPA	610	10.2[a], 17.9[b]	29.7 (–)	
dfppyBPCz	516	19.1[a], 24.4[b]	49.7 (–)	
dfppyBCzP	529	16.8[a], 49.6[b]	60.1 (0.9763); 2767.6 (0.0237)	-2.20
		In CH_3CN		
fppyBTPA	653	0.8[a], 0.8[b]	2.5 (–)	
fppyBPCz	561	4.8[a], 24.0[b]	72.9 (–)	
fppyBCzP	557	7.3[a], 16.8[b]	35.1 (–)	
dfppyBTPA	670	0.4[a], 0.5[b]	0.6 (–)	
dfppyBPCz	551	2.8[a], 6.6[b]	33.0 (–)	
dfppyBCzP	570	6.4[a], 14.1[b]	26.4 (–)	

[a] measured in aerated solution. [b] measured in degassed solution. [c] (–) indicates that the emission can be fitted solely by a single exponential decay kinetics.

Table S8. Thermal analysis of **fppyBTPA**, **fppyBPCz**, **fppyBCzP**, **dfppyBTPA**, **dfppyBPCz**, and **dfppyBCzP**. [a] Temperature at 5% weight loss to initial weight.

	fppyBTPA	**fppyBPCz**	**fppyBCzP**	**dfppyBTPA**	**dfppyBPCz**	**dfppyBCzP**
T_g (°C)	140	135	146	137	142	124
T_d (°C)[a]	392	352	316	359	267	307

Table S9. Electrochemical properties and calculated bandgaps of **fppyBTPA**, **fppyBPCz**, **fppyBCzP**, **dfppyBTPA**, **dfppyBPCz**, and **dfppyBCzP**.

Complex	$E_{1/2}^{ox1}$ (V)[a]	E_{pc}^{re} (V)[a]	HOMO (eV)		LUMO (eV)		Bandgap (eV)	
			CV[b]	DFT	CV[b]	DFT	CV	DFT
fppyBTPA	0.29	-2.45	5.09		2.35		2.74	
fppyBPCz	0.80	-2.46	5.39		2.32		3.07	
fppyBCzP	0.62	-2.43	5.42		2.37		3.05	
dfppyBTPA	0.31	-2.35	5.11		2.45		2.66	
dfppyBPCz	0.79	-2.37	5.39		2.43		2.96	
dfppyBCzP	0.65	-2.37	5.45		2.43		3.02	

[a] $E_{1/2}^{ox1}$ and E_{pc}^{re} are the anodic and cathodic peak potentials referenced to the Fc^{+}/Fc couple. [b] HOMO = $| -4.8 - E_{1/2}^{ox1} |$, LUMO = $| -4.8 - E_{pc}^{re} |$.

Table S10. EL parameters of the **fppyBTPA** and **dfppyBTPA** based OLED devices with different doping concentrations.

DEVICE	CONC.		EQE [%]	CURRENT EFF. [CD · A^{-1}]	POWER EFF. [LM · W^{-1}]
fppyBTPA	4wt%	Peak	12	38.0	37.3
		100 cd · m^{-2}	8.6	27.3	17.2
	8wt%	Peak	20.2	63.9	66.9
		100 cd · m^{-2}	15.5	49.1	28.5
	12wt%	Peak	18.1	57.3	53.0
		100 cd · m^{-2}	13.4	42.3	24.6
	20wt%	Peak	17.2	55.7	46.0
		100 cd · m^{-2}	13.6	44.0	24.7
	25wt%	Peak	16.7	46.4	48.6
		100 cd · m^{-2}	13.4	42.5	23.8
	50wt%	Peak	14	45.5	34.0
		100 cd · m^{-2}	9.7	31.4	15.9
	75wt%	Peak	9.5	29.4	20.1
		100 cd · m^{-2}	4.0	12.4	5.24
dfppyBTPA	4wt%	Peak	14.2	45.7	39.9
		100 cd · m^{-2}	11.8	38.0	22.9
	8wt%	Peak	22.1	63.7	66.8
		100 cd · m^{-2}	18.3	52.8	33.2
	12wt%	Peak	23.4	69.7	68.4
		100 cd · m^{-2}	19.7	58.7	40.1
	20wt%	Peak	25.7	81.6	71.2
		100 cd · m^{-2}	25.4	80.5	63.2
	25wt%	Peak	26.6	88.2	81.5
		100 cd · m^{-2}	25.3	83.9	59.9
	50wt%	Peak	20.5	65.6	64.4
		100 cd · m^{-2}	18.4	58.7	40.1
	75wt%	Peak	15.9	49.6	43.2
		100 cd · m^{-2}	12.4	38.7	24.3

Reference

1. M.-S. Lin, S.-J. Yang, H.-W. Chang, Y.-H. Huang, Y.-T. Tsai, C.-C. Wu, S.-H. Chou, E. Mondal, K.-T. Wong, *J. Mater. Chem.*, 2012, **22**, 16114.

2. W.-L. Tsai, M.-H. Huang, W.-K. Lee, Y.-J. Hsiu, K.-C. Pan, Y.-H. Huang, H.-C. Ting, M. Sarma, Y.-Y. Ho, H.-C. Hu, C.-C. Chen, M.-T. Lee, K.-T. Wong, C.-C. Wu, *Chem. Commun.*, 2015, **51**, 13662.

3. C.-Y. Kuei, W.-L. Tsai, B. Tong, M. Jiao, W.-K. Lee, Y. Chi, C.-C. Wu, S.-H. Liu, G.-H. Lee, P.-T. Chou, *Adv. Mater.*, 2016, **28**, 2795.

4. T.-A. Lin, T. Chatterjee, W.-L. Tsai, W.-K. Lee, M.-J. Wu, M. Jiao, K.-C. Pan, C.-L. Yi, C.-L. Chung, K.-T. Wong, C.-C. Wu, *Adv. Mater.*, 2016, **28**, 6976.

5. Q. Zhang, T. Komino, S. Huang, S. Matsunami, K. Goushi, C. Adachi, *Adv. Funct. Mater.*, 2012, **22**, 2327.

6. T. Nakagawa, S.-Y. Ku, K.-T. Wong, C. Adachi, *Chem. Commun.*, 2012, **48**, 9580.